Solvent effects on photodegradation of the 18-mer of thymidylic acid

An Senior Honors Thesis

Presented in Partial Fulfillment of the Requirements for graduation
with distinction in Chemistry in the undergraduate colleges
of The Ohio State University

by

Eric Daniel Olmon

The Ohio State University
June 2005

Project Advisor: Dr. Bern Kohler, Department of Chemistry

Abstract

The photodimerization of neighboring thymine residues in nucleic acids caused by irradiation of ultraviolet light can lead to harmful mutagenic products. The 18-mer of single-stranded thymidylic acid [$(dT)_{18}$] dissolved in various denaturing solvents was used as a model system to determine the rate of this photoreaction. The maximum percents volume of co-solvent in water/co-solvent mixtures of ethanol, trifluoroethanol (TFE), and dioxane in which the molecule was soluble were determined to be 75%, 100%, and 75%, respectively. Solutions of $(dT)_{18}$ in these solvent mixtures were irradiated with femtosecond pulses of 271 nm light, and UV-Vis absorption and CD spectroscopies were used to monitor the rates of photodimerization. Rates of photodimerization relative to $(dT)_{18}$ in water were determined to be 0.356, 0.258, and 0.439 for the co-solvents ethanol, TFE, and dioxane, respectively. A qualitative relationship was found between the amount of base stacking observed in the non-irradiated solutions and the rate of photodimerization for solutions containing ethanol and TFE, but this relationship did not hold for dioxane.

Contents

List of Figures

List of Tables

Chapter 1

Introduction

The excitation of a thymine residue of DNA by a photon of ultraviolet light has the potential to bring about a photoreaction in DNA that leads to mutation, mis-transcription, and propagation of an error in the genetic code to generations of daughter cells.[1] Every organism from *Esherichia coli* to *Homo sapiens sapiens* utilizes an elaborate system of maintanence and repair enzymes to prevent and undo the damage done on DNA by sunlight.[2] The particular photoreaction of interest in this study involves two neighboring thymine residues on a nucleic acid chain which undergo a photodimerization reaction upon the absorption of ultraviolet light. It is our hypothesis that the incidence of the photodimerization reaction is dependent on the extent of base stacking in the oligonucleotide.

This study focuses on the photoreaction of a specific nucleotide, the single-stranded 18-mer of thymidylic acid, abbreviated as $(dT)_{18}$. This molecule is of particular interest because pyrimidines such as thymine are considerably more sensitive to irradiation than purines, and the photodimerization of adjacent thymines in a DNA strand can eventually lead to the loss of replicative function in a cell.[1] Finally, the advantage of using a custom-synthesized oligomer instead of a natural DNA is that it is a very well-defined model system, in contrast to the polymer systems of the past which had various and undefined compositions and lengths.

1.1 Goals of this study

In the present study, we examine the mechanism of thymine-thymine photodamage in a short oligonucleotide. By studying differences in the circular dichroism of $(dT)_{18}$ solutions with changes in the denaturing ability of solvents and in irradiation times, we will show that there is a correlation between the amount of stacking in the bases and photodimerization. Using this oligonucleotide, we hope to build upon the research and knowledge that has come before us.

This thesis is broken up into two related parts. The first deals with the solubility of $(dT)_{18}$ in different solvents, and the second deals with irradiation of $(dT)_{18}$ in these solvents. Both dependencies are monitored by steady state absorbance and circular dichroism measurements. The experimental methods and results will be described after reviews of nucleic acid concepts, literature, and instrumentation.

1.2 Nucleic Acids

Before we begin analyzing experimental results, it is necessary to review some basic nucleic acid chemistry and general photophysics and photochemistry so that we may effectively analyze the data. The following short history will review the discoveries of the various components and structures of nucleic acids and the nomenclature of the field. Further information will provide descriptions of attractive interactions in nucleotides, the mechanics of electronic excitation, and the photodimerization of thymine.

1.2.1 Early studies on the structure of nucleic acids

In the late 1940s and early 50s one published paper after another furthur elucidated the mysterious nature of DNA, fitting large jigsaw pieces into the puzzle of evolution. Oswald Avery, a bacteriologist and research physician, proved in 1944 that DNA—

rather than various proteins, as had been the common hypothesis previously—was the molecule responsible for the transfer of genetic information from one generation to another.[3] Naturally, this discovery led to much curiosity as to the mechanism of the process, and therefore also to the structure of the molecule itself.

The discovery of nucleic acids began long before Avery's experiments. In the latter half of the nineteenth century, Johann Friedrich Miescher isolated a gelatinous material that he called *nuclein* from the nuclei of lymphoid cells and showed that it contained organic phosphorus.[4] A few years later, Albrecht Kossel discovered that nuclein contained four organic bases—adenine, guanine, thymine, and cytosine—work for which he was awarded a Nobel prize,[5] and Altman deproteinized the nuclein of yeast and called the product nucleic acid.[6] In 1891, Kossel found a sugar in nucleic acid[7] that was later identified as D-ribose by Levene and Jacobs in 1908,[8] and in 1901 another base called uracil was discovered by Ascoli.[5] With the identification in 1929 by Levene of 2′-deoxy-D-ribose,[9] all the components of DNA had been found.

The structures of these components are shown in Figure 1.1, in addition to the deoxyribonucleotide monomer of thymine, thymidylate. The discovery of organic phosphate was novel at the time; before Miescher's work, it had only been found in the phospholipid lecithin.[5] Organic phosphate commonly forms ester linkages (a chain of bonds through the oxygen atoms) with other organic molecules.[10] The nomenclature of 2′-deoxy-D-ribose indicates that a hydroxyl (-OH) group is missing from the second (2′) carbon, and that a solution of the sugar will rotate a plane or polarized light counterclockwise; the D designation, which stands for *dextrarotatory*, is used to distinguish the molecule from L-ribose, which will rotate a plane of polarized light clockwise (*levorotatory*). Ribose is a five-carbon sugar, in this case known as a furanoside because it is cyclized into a five-membered oxygen-containing ring similar to the molecule furan.[10] Scientists knew the structures of the components of DNA by 1929, but it was not until twenty years later that the functions of the components were explained.

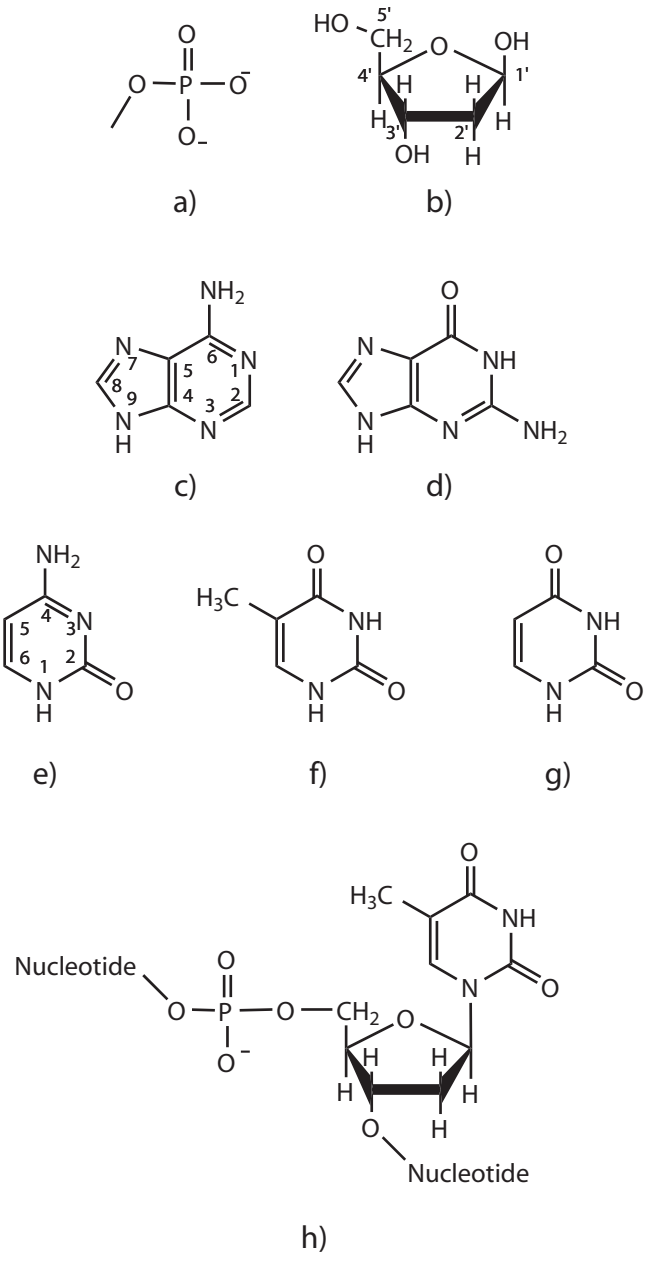

Figure 1.1: The components of nucleic acids; a) phosphate, b) 2′-deoxy-D-ribofuranose, c) adenine, d) guanine, e)cytosine, f)thymine, g) uracil, h) thymidylate.

The research of Erwin Chargaff and Ernst Vischer at the end of the 1940s provided a very valuable insight into the nature of DNA. Vischer had been given the task of separating the bases from the DNA of various organisms in an effort to establish a parallel between taxonomic relationship and DNA composition.[11] What he and Chargaff found instead was that the ratios of adenine to thymine and guanine to cytosine in the DNA of all the organisms studied was unity.[12] The testing methods were perfected and the conclusion was annouced by Chargaff at a series of lectures given throughout Europe in June of 1949 and in the Swiss journal *Experientia*.[11,13] The one-to-one relationships between adenine and thymine, and guanine and cytosine have come to be known as Chargaff's rules.[14]

The earliest structural studies of intact DNA were made using X-ray crystallography. This method uses X-rays diffracted from various layers of a crystal structure of a molecule to probe its electron density. Once the crystal structure of a molecule is known, potential energies, which indicate conformational flexibilities within the molecule, can be calculated from this information.[15] DNA and RNA, however, provide a particular challenge in x-ray crystallography. Due to the large number of conformations in these long molecules, single crystals cannot be obtained , and structural analysis cannot be carried out to great detail.[16] This lead to various interperetations of crystallographic data and much correspondence between scientists in the early 1950s.

James Watson and Francis Crick proposed the correct general structure of DNA in 1953. In a famous 1953 letter to *Nature*, they annouced their dissatisfaction with a structure proposed earlier that year by by Linus Pauling and Robert Corey,[17] which suggested that three deoxyribose chains wind around a central axis of phosphates with the various bases on the outside of the molecule.[18] Instead, they favored an extention of Furberg's "standard configuration,"[19] with the bases on the inside of the helix and the phosphates on the outside. The novel difference between Watson's and Crick's structure and earlier proposals was the insight that two helices were involved, held together by

hydrogen bonding between pairs of bases. Furthurmore, by pairing the bases in the manner elucidated by Chargraff[13] and Wyatt,[20] a copying mechanism for DNA became apparent.

1.2.2 The current view of DNA and RNA

The current view of DNA is shown in Figure 1.2. The carbon atoms of the deoxyribose

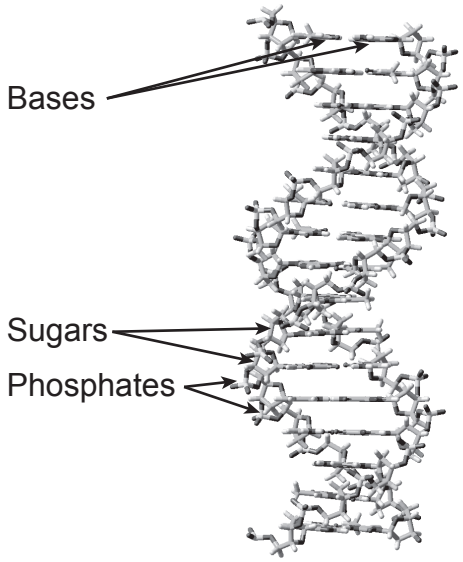

Figure 1.2: The structure of B-form DNA.

units are numbered according to IUPAC (International Union of Pure and Applied Chemistry) specifications: as sequential numbers each followed by a prime ($'$) symbol. A symbol α or β is used to describe the sugar-phosphate linkage. Nucleic acids are made of two long strands, each of β-deoxyribofuranosides joined by $3'$-$5'$ phosphate diester linkages. These strands run antiparallel (one strand goes from $3'$ to $5'$ while the other goes from $5'$ to $3'$) and wind around a central axis in the form of a double helix, with the bases covalently bonded to the sugar units at the $1'$ position and hydrogen-bonded to each other.[10]

Ribonucleic acid, or RNA, while biologically much more complex than DNA, is very

similar to DNA in structure. Rather than two phosphate-sugar strands forming a double helix, RNA is composed of only one phosphate-sugar strand. Because of this, RNA can form various biologically-useful structures when complimentary bases at different parts of the molecule hydrogen-bond with each other. The sugar units of RNA do not lack their 2′ hydroxyl (-OH) groups (hence *ribonucleic* rather than *deoxyribonucleic*). Also, RNA contains the base uracil instead of thymine. The two bases have the same structure except that uracil lacks a methyl group on carbon-5.[10]

1.2.3 The nucleic acid bases

Figure 1.1 shows the four DNA bases—adenine, thymine, cytosine, and guanine—and the additional RNA base uracil. The bases can be categorized by their central ring structures: adenine and guanine are bicyclic purine derivatives, while thymine, cytosine, and uracil are unicyclic six-membered pyrimidine derivatives. All of the nucleic acid bases are aromatic, meaning they contain systems of delocalized electrons, resulting in planar structures and absorptive properties. The bases are also heterocyclic, meaning they contain atoms other than carbon in their central ring structures. These two structural features are necessary for the two types of forces that are responsible for the cohesive nature of DNA: hydrogen bonding and base stacking.

1.2.4 Hydrogen bonding and base stacking

Hydrogen bonds are relatively weak non-covalent interactions of the type

$$\mathrm{X} - \mathrm{H} \cdots \mathrm{Y} \tag{1.1}$$

where a hydrogen atom is connected covalently to X, usually carbon, and connected to Y, an electronegative atom such as oxygen, nitrogen, or sulfur, by a hydrogen bond. The hydrogen bond interaction arises because as X pulls electrons away from H, Y

becomes more attracted to the relatively positive nature of H. Hydrogen bonds in general are well-defined neither in length nor direction. The bond length depends on the electronic environment of X and Y, and the attractive force does not project strictly linearly with the X − H bond, leading to some variation in the types of structures that can be stabilized by hydrogen bonds. Hydrogen bond interactions are also 20 to 30 times weaker than covalent bonds.[16] The hydrogen bonding between the bases is very effective as a result of the planarity and heterocyclic nature of the molecules. These properties cause multiple amine and keto substituents to line up with hydrogen atoms on comlimentary bases to ensure just the right amount of interaction—enough to hold the DNA together, but not enough to prevent it from being broken apart under the right conditions. The common Watson-Crick base pairing is shown in Figure 1.3.

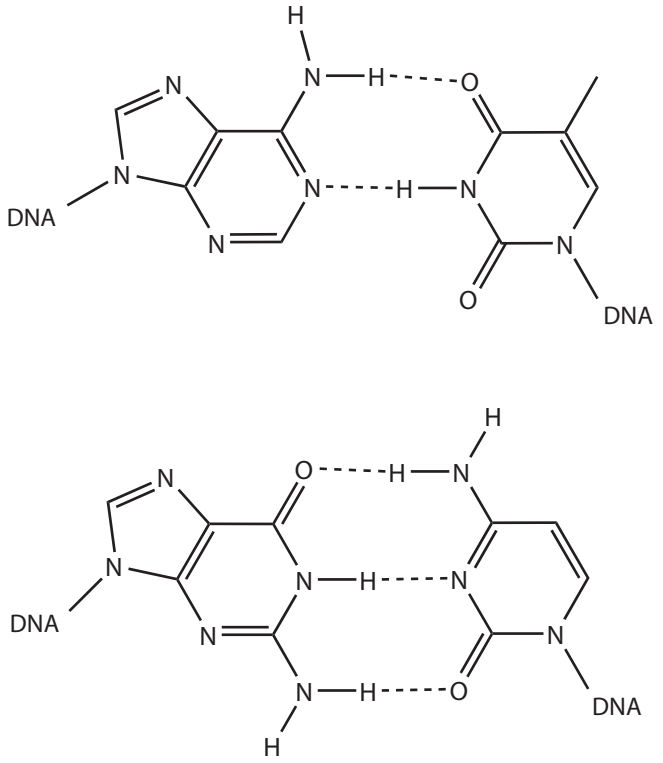

Figure 1.3: Common Watson-Crick pairing in hydrogen-bonded bases of DNA; the top pair is adenine and thymine and the bottom pair is guanine and cytosine.

While horizontal hydrogen bonding arrangements are observed almost exclusively in non-aqueous solutions and in the gas phase, vertical interactions known as base stacking, or self-association, are preferred in aqueous solutions over hydrogen bonding. The bases aggregate so that their molecular planes lie parallel, in columns that can contain two or more bases.[15] In many cases, the polar substituents of one molecule (–NH_2, =N–, or =O) will lie directly over the aromatic system of the other.[16] The extent of base stacking varies depending on the bases involved, with pyrimidines such as thymine, uracil, and cytosine showing less stacking character than purines such as adenine and guanine.[21]

1.2.5 Thermodynamics of base stacking

Because base stacking is only observed in strong hydrogen bonding solutions, it is apparent that the nature of the solvent is responsible for the shift in stability from horizontal hydrogen bonding to vertical base stacking. Thermodynamic data in Table 1.2.5 show that negative enthalpy and entropy changes (ΔH and ΔS, respectively) are involved in all base stacking interactions.[21] Changes in free energy (ΔG) were calculated using the thermodynamic relation

$$\Delta G = \Delta H - T\Delta S \tag{1.2}$$

where T is the temperature of the system. The K values, which represent association constants, are characteristic of weak interactions.[16]

The table conveys three important points. First, base stacking in polar solvents can lead to negative ΔG values, proving that base stacking is a thermodynamically favorable process; second, purines show more negative energies of base stacking than pyrimidines; and third, methylation leads to a more negative ΔG, as shown by the difference in ΔG between 6-methylpurine and purine.

Compound	K(25°) [l/mole]	ΔH(25°) [kcal/mole]	ΔS [e.u.]	ΔG [kcal/mole]
6-Methylpurine	6.7	-6.0±0.4	-16	-1.12
Purine	2.1	4.2±0.2	-13	-0.44
Ribosylpurine	1.9	-2.5±0.1	- 7	-0.38
Deoxyadenosine	4.7 to 7.5	-6.5±1.0	-18	-1.00
Cytidine	0.87	-2.8±0.1	-10	0.08
Uridine	0.61	-2.7±0.1	-10	0.29
Thymidine	0.91	-2.4±0.3	- 9	0.06

Table 1.1: Thermodynamic Data of Nucleoside and Base Stacking in Water; From Ts'o, 1974.

The first point has been explained by a phenomenon common in biochemical macromolecules called hydrophobic (literally "water fearing") interactions. When a single hydrophobic molecule (a nonpolar molecule) is placed into a polar solvent such as water, solvent molecules will try to avoid it, forming a structured water cluster around it and causing a decrease in entropy (an unfavorable process), which is proportional to the surface area of the hydrophobic molecule.[22] If a second hydrophobic molecule is added to the solution, it will tend to aggregate with the first molecule because the surface area of two aggregated molecules is less than the surface area of two separate molecules, leading to less of a decrease in the entropy of the system. Although the negative entropy change shown in Table 1.2.5 indicate an overall unfavorable process, some studies[23,24] have explained that a "hidden" positive entropy change associated with the actual base stacking is masked by other effects.[16]

The second and third points are explained by London dispersion forces and interactions between dipoles.[16] A dipole is a permanent electric moment in a molecule caused by a difference in the electronegativities of the atoms (one end of the molecule will have more positive character while the other end of the molecule will have more negative character). London dispersion forces are due to fluctuations in the electronic charge distribution of a molecule. When electrons shift to one end of a molecule, a temporary dipole is created which causes a similar shift of electrons in neighboring molecules and

an attraction between the two.[25] The strengths of the electronic interactions between two bases is related to the structure and composition of the bases. These effects are stronger for purines and methylated bases in polar solvents than for pyrimidines and unmethylated bases, respectively.[16]

1.2.6 Base stacking in oligo- and polynucleotides

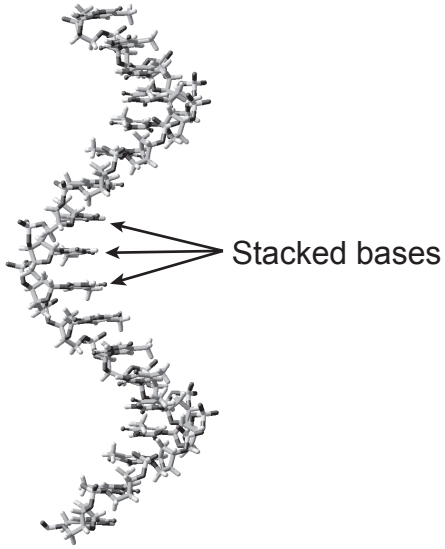

Figure 1.4: Ideal base stacking in $(dT)_{18}$.

Nucleic acid bases in polynucleotide chains show the same stacking trends as those mentioned above. Nucleic acids made mostly of purines like adenine show large amounts of stacking in water solutions, which leads to a more stable chain and the formation of a single helix; nucleic acids made mostly of pyrimidines, on the other hand, show much less stacking, and predominate as random coils rather than stabilized helices at room temperature.[26] It has been shown[26–28] that the change between the helical and random coil conformations can be described kinetically by a simple two-state process:

$$\text{helical(stacked)} \rightleftharpoons \text{randomcoil(unstacked)} \tag{1.3}$$

in which the methylation and ring structure of the bases largely determine the direction of equilibrium. Although the stacking interactions of pyrimidines such as thymine are not as strong as those of purines, pyrimidines do stack to some extent when placed into an aqueous solvent. In the ideal case, this base stacking gives oligo- and polynucleotides the helical secondary structure as shown in Figure 1.4. For this study, we have assumed that thymine base stacking is described by this two-state process: the bases are thought of as having either stacked or unstacked conformations, but not intermediate conformations.

1.2.7 Electronic excitation in molecules

The energy of atoms and molecules is quantized, so energy can only be gained or lost in discrete amounts.[29] The possible energy states of an atom or molecule are often represented by an energy level diagram, as shown in Figure 1.5, where the thick horizontal lines indicate possible energy magnitudes for the electrons of the molecule and the thin horizontal lines indicate possible molecular vibrational energies. This

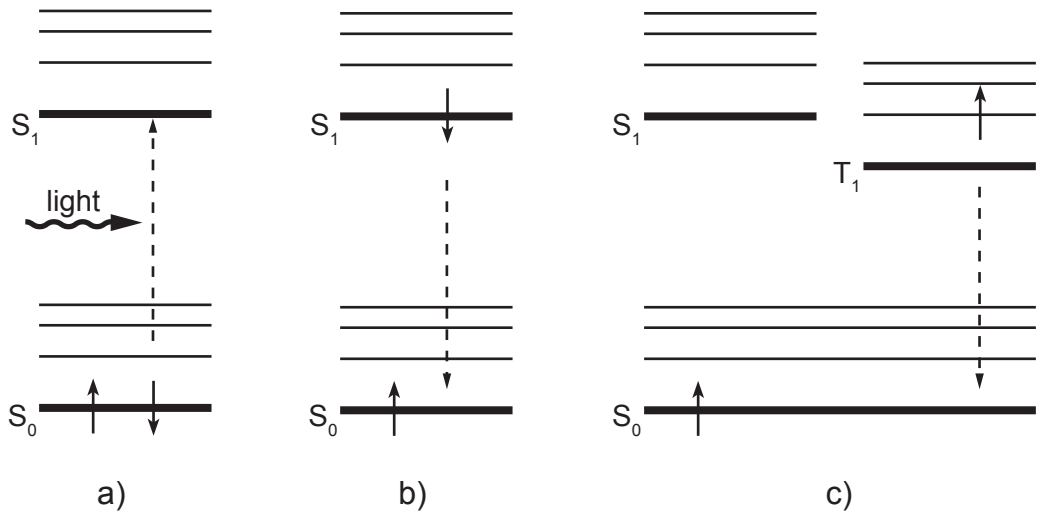

Figure 1.5: A Jablonski energy level diagram; a) absorption, b) fluorescence, c) phosphorescence.

simplified energy diagram shows a) an absorption from the S_0 state to the S_1 state; b) fluorescence emission back to the S_0 state, and c) phosphorescence emission from the T_1 to the S_0 state. The conversion from the S_1 to the T_1 state is known as intersystem crossing and involves a change in the spin quantum number. Since no two electrons can have the same four quantum numbers, the spin quantum number of an electron in the T_1 state must change again before it can relax to the ground S_0 state. Because of this, the T_1 is a much longer-lived state than the S_0 state. Possible molecular rotational energies, which are not shown in the diagram, have even smaller spacings than vibrational energies.

When a molecule is excited, its electrons will jump from a lower level to a higher level, and the distance of the jump is equal to the amount of incoming excitation energy.[29] One of the most common sources of excitation energy is electromagnetic radiation. The energy of light is related to its frequency and wavelength by two forms of the Plank equation:

$$E = h\nu \tag{1.4}$$

$$E = \frac{hc}{\lambda} \tag{1.5}$$

where E is the energy, h is Plank's constant (6.626×10^{-34} J s), c is the speed of light in vacuum (2.998×10^{8} m s^{-1}), ν is the frequency of the incoming light, and λ is the wavelength of the incoming light.[29] In order for an energy transition to occur, the energy of the incoming radiation must be equal to the difference in energy between the initial energy state of the molecule and the excited energy state of the molecule.[29] If the excitation energy matches the difference in energy between two energy states, an absorption will occur, and the energy of the molecule will increase.

1.2.8 The photodimerization of thymine

Thymine residues undergo electronic transitions when they are excited by ultraviolet light. Upon absorption, an electron will be promoted to the S_1 electronic state. From there, it can relax back to the ground S_0 state through fluorescence or it can undergo intersystem crossing to a vibrational mode of the T_1 state, where it can phosphoresce to the S_0 state. The fluorescence lifetime for thymine oligomers is ultrafast as shown by Marguet[30] and Crespo[31] while phosphorescence is a much slower one.[32]

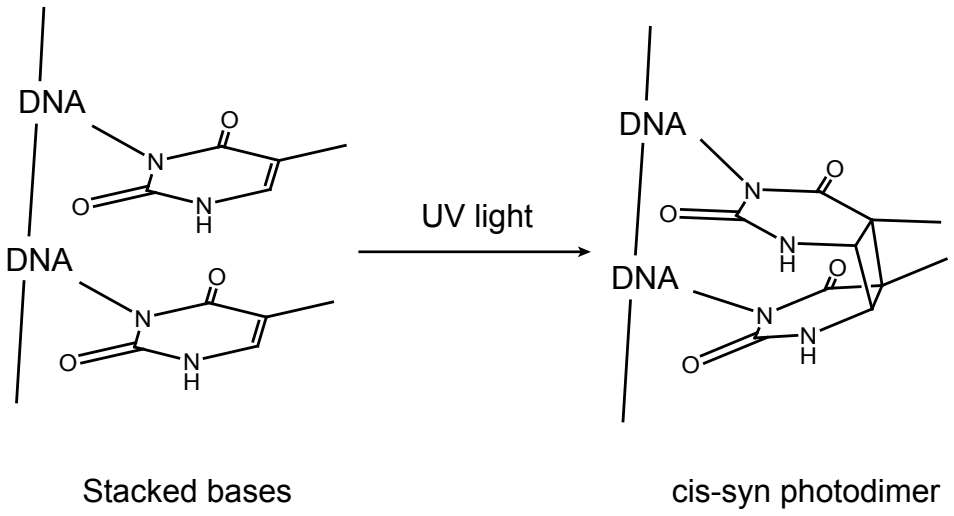

Figure 1.6: The photodimerization reaction in nucleic acids.

An excited thymine residue has the potential to form a photodimer with a neighboring thymine residue[33] by the cycloaddition reaction shown in Figure 1.6. Free bases in solution can form four different photodimer isomers, but thymines bonded to a nucleotide chain can only form the *cis-syn* structure shown in Figure 1.6. It is this photodimer which is responsible for the loss of replicative function in cells.[1]

1.3 Hypothesis

Our hypothesis is that photodimerization is dependent on base stacking. The excited state characteristics of thymine make this very reasonable. We know photodimers are formed and we assume that the conformation of the oligomer can be described as either stacked or unstacked. It is evident from the rotational spectroscopy data of various molecules that the frequency of rotation around a single bond for many bonded atom pairs is greater than one microsecond. It can therefore be assumed that the period of rotation involved in the change from a stacked to an unstacked conformation in $(dT)_{18}$ is probably greater than one microsecond. Marguet's and Crespo's data show that the relaxation of excited thymine is ultrafast; that is, thymine relaxes from an S_1 state rather than a T_1 state. Since it takes more time to switch from an unstacked conformation to a stacked conformation than for the molecule to relax by fluorescence, it is our hypothesis that the bases must be stacked in order for photodimerization to occur.

1.4 Review of related research

Over the past fifty years, countless experiments have been performed, millions of dollars have been spent, and many years of many scientists' lives have been devoted to understanding exactly how these biological processes function and how DNA becomes damaged. Soon after the first observation in 1958 by Rörsch *et al.*[34] that far-UV absorption could lead to stable photoproducts in nucleic acids, the thymine photodimer (T<>T) was isolated and characterized.[35,36] It was shown that the photoreaction could be reversed by exposing the photoproduct to 254 nm light.[36] Research by Beukers[33] and Wacker[37] showed that the thymine photodimer , particularly the *cis-syn* isomer, is a major far-UV lesion in DNA. This discovery led to numerous studies related to the

formation and structure of light-induced pyrimidine dimers in general, as reviewed by Fahr[38] and Fisher and Johns.[39] Some of these studies showed that pyrimidine dinucleoside monophosphates undergo very efficient photodimerization in aqueous solutions at room temperature.[40–45] More recently, the photoreactive properties of derivatives of nucleic pyrimidine bases have been studied, showing that photodimers are not unique to the pyrimidine bases.[46] Also, research has shown that the creation of photodimers can induce conformational changes in DNA.[47,48]

Circular Dichroism (CD) spectroscopy has been used to monitor changes in the secondary structure of DNA and RNA strands as a function of pH, solvent, and temperature. Measurements of the CD of various deoxynucleosides and deoxydinucleotides were published by Cantor and Warshaw in 1970.[49] In 1973, Girod *et al.* showed that the CD spectrum of calf thymus DNA decreases with increasing ethanol concentration in aqueous solutions,[50] and in 1977 Pettegrew showed that CD signal of the adenine dimer decreases with increasing percent volume of dioxane in water/dioxane mixtures.[51] In 1986, Steely showed that the CD spectra for the nucleic acid polymers of ribouracil, deoxyribouracil, and deoxyribothymine are very similar because of the similar and minimal amount of base stacking exhibited by the three.[52]

Much work has also been done to determine the lifetimes of the excited states of various nucleic acid bases. In solutions of less than 10^{-2} M thymine monomers, where no ground state associations occur between base molecules, the longer-lived triplet excited state (T_1) rather than the singlet state (S_1) is the reactive intermediate,[53] and the quantum yield of the thymine dimers is on the order of 0.001.[54] As the concentration of base is increased, self-associative attractions known as base stacking become prominent. In solutions of base-stacked dimethylthymine (DMT), Lisewski and Wierzchowski have shown that high concentrations of triplet quenching molecules are ineffective at quenching the dimerization of the bases, providing evidence that the photodimerization reaction occurs through the S_1 state.[55] At an infinite concentration of DMT the

quantum yield has been calculated as 0.125.[55] When the same tests were carried out in organic solvents, dimer quantum yields decreased, suggesting that organic solvent molecules disrupt associations between the pyrimidines.[56] Several researchers have shown that the quantum yield of pyrimidine photodimers in thymine and uracil dinucleotides, and in random-sequence oligonucleotides, polynucleotides, and DNA is about 0.01.[40,41,44,57–60] More recent nanosecond transient absorption studies by Marguet[30] show that the quantum yield of T<>T in $(dT)_{20}$ is $(2.8\pm0.2)\times 10^{-2}$ and that the fluorescence upconversion lifetime of $(dT)_{20}$ is 0.3 ps at 330 nm,[61] which is six orders of magnitude faster than the lifetime of the triplet state (about 10^{-6} seconds[32]). Crespo *et al.* have used femtosecond transient absorption in the visible range to show that the fluorescence lifetimes of the 18-mer at a probe wavelength of 570 nm is 0.74(6)ps.[31] The lifetime determined by Marguet and Crespo differ by a factor of two, perhaps because of some influence by the technique used. However, both of these studies prove that the fluorescence is ultrafast.

Calculations on photodimer formation have supported experimental conclusions. Durbeej and Eriksson have used computational techniques to investigate the formation of thymine dimers in DNA, showing that the calculated vertical excitation energy corresponding to the singlet transition lies in the far-UV region, in accordance with experimental data.[62] Further calculations have also shown that T<>T is the most common photodimer formed in DNA due to the presence of an excited-state energy minimum, which is not found in the excited states of other bases.[63]

Chapter 2

Instrumentation

2.1 Principles of absorption spectroscopy

The two main techniques used in our experiments were steady state molecular absorption and circular dichroism (CD) spectroscopies. In steady-state absorption spectroscopy, the electrons of a molecule are excited from the ground electronic state to an excited electronic state. The wavelength of the excitation radiation is scanned in the ultraviolet or visible range and the difference in transmission is observed versus wavelength between light traveling through the sample of interest and light traveling through a blank sample. CD spectroscopy is very much like absorption spectroscopy, except that the incident light in CD spectroscopy is circularly-polarized. Due to the nature of circularly-polarized light, absorption of this light by chiral molecules is selective for one polarization or another. By examining the difference in absorption between left-circularly-polarized light and right-circularly-polarized light, it is possible to deduce certain characteristics of the structure of a sample molecule.

2.1.1 Polarization of light

Light propagates through space as a wave with an electric field component and a magnetic field component that are orthogonal to each other, a characteristic frequency that is proportional to the energy of the light, and a constant velocity in vacuum. For ease of understanding the concepts involved, only the electric component will be considered further. This component, represented henceforth as **E** can be described generally as a vector in time and space which is perpendicular to and free to rotate around a line describing the propagation of the light wave in space. Linearly-polarized light is light for which this vector is restricted from rotation around the line of propagation. The wave nature of the light is exhibited by the changing amplitude of this vector, which oscillates sinusoidally in time.

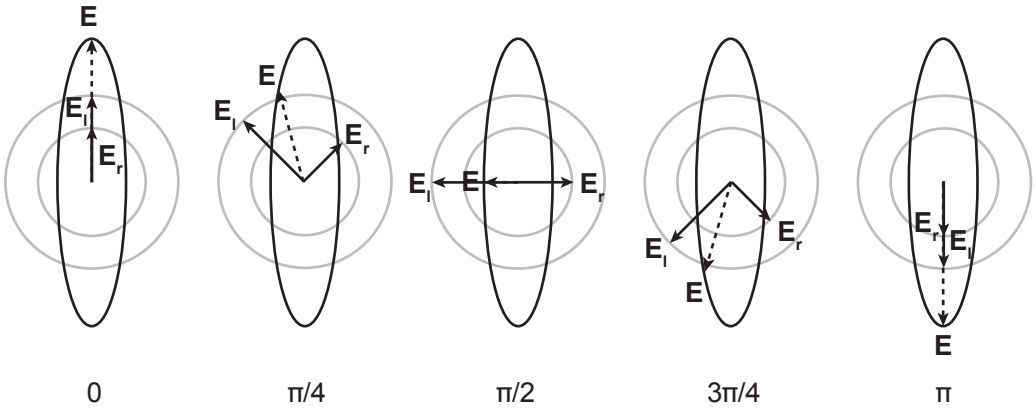

Figure 2.1: A vector diagram of elliptically-polarized light.

The polarization of light can be described geometrically. The electric field vector of light is represented by the sum of vectors representing two colinear beams—a right-circularly-polarized beam, $\mathbf{E}_r$ and a left-circularly-polarized beam, $\mathbf{E}_l$—which are perpendicular to the line of propagation and rotate around it in opposite directions and at equal rates.[64] If the two vectors are equal in magnitude, the addition of the two vectors will result in linearly polarized light. If the two vectors have different magnitudes,

elliptical polarization will result. This condition is shown in Figure 2.1. If one vector has zero magnitude, only the other vector will remain, resulting in circular polarization.

2.1.2 Molecular absorption

Experimentally, absorbance is measured as the amount of light that does not hit a detector. That is, light of a given wavelength is passed through a standard—usually the solvent without the analyte—and its intensity is measured. Then light of the same wavelength is passed through a sample—the solvent with the analyte—and its intensity is measured. The quotient of these two intensities is known as transmittance, and is usually reported as a percent:

$$T = \frac{P}{P_0} \times 100 \tag{2.1}$$

where T is the transmittance, P is the intensity of light after absorption by the sample, and P_0 is the intensity of the light before absorption.[65] Often, the relationship between P and P_0 is more usefully reported as absorbance:

$$A = log\frac{P_0}{P} \tag{2.2}$$

or

$$A = \epsilon bC \tag{2.3}$$

where ϵ is known as the molar absorptivity constant, b is the pathlength of the sample cell in cm, and C is the concentation of the sample in mol L^{-1}.[65] Equation 2.3 is known as the Beer-Lambert law. Absorbance is unitless, so the units of the molar absorptivity constant are cm^{-1} M^{-1}. The molar absorbtivity is dependent on the effective cross section of the sample molecules in solution and on the probability that the impact of a photon will lead to a transition, which itself depends on the orientation of the molecule, on the wavelength of the incoming light, and on the nature of the solvent.[65] Due to the

complexity of calculating this constant, it is usually determined empirically.[65] Because the molar absorptivity is dependent on wavelength, so is absorbance.

2.1.3 The quantitation of circular dichroism

Circular polarization has been described in terms of the addition of two vectors, $\mathbf{E}_l$ and $\mathbf{E}_r$. Since $\mathbf{E}_l$ and $\mathbf{E}_r$ have different indeces of refraction in some substances, it is reasonable to expect them to have different molar absorptivity constants in these substances. The difference between the two molar absorptivity constants is called circular dichroism (CD), and is expressed

$$\Delta\epsilon = \epsilon_l - \epsilon_r, \tag{2.4}$$

where ϵ_r is subtracted from ϵ_l, rather than the other way around, by convention. If a plane-polarized beam of light (thought of here as a sum of two circularly-polarized beams) enters a sample that is CD-active, the right-polarized beam and left-polarized beam will be absorbed to different extents, leading to elliptically-polarized light. This effect can be represented by the Beer-Lambert law as

$$\begin{aligned} \Delta A &= A_l - A_r & (2.5)\\ &= \epsilon_l bC - \epsilon_r bC & (2.6)\\ &= \Delta\epsilon bC & (2.7) \end{aligned}$$

The CD effect is measured by quantifying the ellipticity, θ, which is the inverse-tangent of the ratio of the minor and major axes of the ellipse, and is related to circular dichroism by

$$\theta(radians) = (2.303\ C'\ b'/4)\Delta\epsilon \tag{2.8}$$

The factor 2.303 compensates for a logarithm conversion between base 10 and base e, and C' and b' are measured in mol L^{-1} and cm, respectively. A more common measure for solution chemsitry is molar ellipticity in L mol^{-1} cm^{-1},

$$[\theta](\lambda) = \frac{100\theta(\lambda)}{b\,C} \tag{2.9}$$

where b is in cm, C is in mol L^{-1}, and 100 is a historical constant. The molar ellipticity is related to the circular dichroism by

$$[\theta] = 3298\Delta\epsilon \tag{2.10}$$

and both units are commonly used to report CD effects.[64]

2.2 The link to biochemistry

The natural world has evolved such that chirality is a crucial characteristic of biomolecules. For example, sugars are almost always found in the D form, and amino acids are almost always in the L form.[10] Because of this, many biological molecules are CD active, and as was shown in the introduction, much useful information has been gained by exploiting this chirality to our advantage in CD experiments.

Chapter 3

Experimental methods

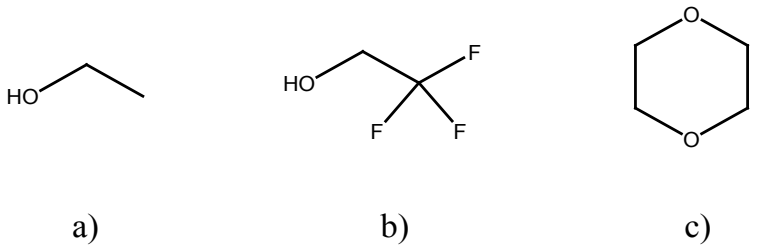

Figure 3.1: Structures of the solvents used; a) ethanol, b) TFE, and c) dioxane.

Throughout the study, we used deionized 25 mM phosphate buffer at neutral pH rather than pure water. The co-solvents were reagent-grade ethanol, trifluoroethanol (TFE), and dioxane. The chemical structures of the co-solvents are shown in Figure 3.1. We purchased the solvents from various chemical suppliers. We used these particular solvents because they are commonly used to denature double-stranded DNA. Their denaturing effectiveness has to do with their hydrophobic character relative to water. Rather than destabilizing the helical form of a nucleotide, they stabilize the exposed bases of the ahelical form[66]—the bases, which tend to aggregate in an aqueous solution, are stabilized in nonpolar solutions by solvent shells, which are free to form around them. We purchased the $(dT)_{18}$ from Midland Certified Reagent Company (Midland, Texas,

USA). The samples arrived in small plastic vials, each containing 33.8 nmol (183.30 μg) of lyophilized powder $(dT)_{18}$. This quantity was indicated by the labels on the vials, which were not opened until we were ready to dissolve the samples. We measured absorbance using a Perkin Elmer Lambda 25 double-beam UV-Vis spectrophotometer, and we measured CD using an AVIV model 202 circular dichroism spectrophotometer.

3.1 Solubility experiments

Ideally we would carry out the radiation studies in solutions of pure solvents since our goal is to show the effects of various solvents on the formation of the photodimer. However, $(dT)_{18}$ is insoluble in many pure solvents. In order to increase solubility while still observing solvent effects on the system, we mixed the solvents of interest (from now on referred to as "co-solvents") with water. We wanted to use the highest concentrations of co-solvents in co-solvent/water mixtures in which $(dT)_{18}$ was soluble in order to maximize the denaturing effect of each co-solvent while still achieving solubility. The magnitude of the absorbance maximum was used to determine the solubility.

In the first solution we made, we used buffered water as the solvent. Next we made a series of solutions with varying percents volume of co-solvent in aqueous phosphate buffer. For ethanol, we made solutions of 25%, 50%, 75%, and 100% volume ethanol. The TFE/water percents volume were also 25%, 50%, 75%, and 100% . Due to the nonpolar nature of dioxane, we assumed that $(dT)_{18}$ would be insoluble at a lower volume percent in dioxane than in the other two co-solvents. Therefore, we initially made solutions of 10%, 25%, 50%, and 75% volume dioxane. When we found that $(dT)_{18}$ dissolved readily in the 75% mixture, we made a fifth sample of 100% volume dioxane, but $(dT)_{18}$ was insoluble in this sample. All of the solvents were visibly transparent except the 75% mixture of ethanol. We do not know the reason for the translucency of the 75% ethanol solution, but we will spend time in the future to figure this out.

To prepare the samples, we added a 0.500 mL aliquot of the above-mentioned solvent mixtures to each of fourteen plastic vials (one water sample, four ethanol samples, four TFE samples, and five dioxane samples) containing $(dT)_{18}$. We shook the vials gently for five minutes to ensure complete solvation.

We used a 1.0 mm quartz cell to take absorbance and CD measurements. The CD spectra were taken to ensure that the samples were CD-active at every percent composition that showed an absorbance signal. For both techniques, we corrected each measurement for solvent background with a 1.0 mm reference cell containing the appropriate co-solvent/water mixture. We used a scan range of 400 nm to 200 nm with a constant bandpass of 1.0 nm and a scan rate of 1 nm s^{-1}. We kept the temperature of the CD spectrometer constant at 25°C.

3.2 Radiation experiments

The four solvents used in the radiation experiments were phosphate buffer, 50% ethanol, 75% TFE, and 75% dioxane. To prepare the samples, we added a 0.500 mL aliquot of different solvent mixtures to each of four plastic vials containing $(dT)_{18}$. We shook the four vials for five minutes, then transferred the contents of the plastic vials to larger glass vials and diluted the solutions to about 5 mL by adding the appropriate solvent mixture to each vial. This two-part dilution was necessary due to the very small amount of $(dT)_{18}$ used.

It has been shown mathematically that CD measurements are most efficient if the normal absorbance at the absorbance maximum of the sample is 0.869 and that it should not exceed the range of $A = 0.6$ to $A = 1.2$.[64] We diluted the four samples with the appropriate solvents so that their absorbance maxima were similar and were within this range.

Once the solutions were prepared, we made a series of measurements and irradiances.

We placed each solution into a 1.00 cm quartz cuvet with a magnetic stirrer, where it remained for the duration of the experiment. A 1.00 cm cuvet was used rather than a 1.0 mm cuvet as in the solubility experiments in order to accomodate the stirrer. The stirrer was necessary in the radiation experiments to ensure that fresh solution was continuously being pulled into the beam path. We measured the absorbance and CD from 350 nm to 200 nm. During the CD measurement, the sample was stirred. We averaged each CD spectrum over three scans in an effort to reduce shot noise. Finally, we used the output of a tuneable optical parametric amplifier at Ohio State's Center for Chemical and Biophysical Dynamics to irradiate the water sample for a short time. The laser had a wavelength of 271 nm and a beam width of 3.24 mm. We used a neutral density filter to attenuate the power density of the beam to 15.2 mW cm^{-2}, which is a relatively low value. We kept the power density low to prevent interferences that can be caused by the two-photon ionization of water.[31] We repeated this cycle of absorbance measurement, CD measurement, irradiation for the water sample until the measured absorbance was 50% of the original absorbance at 260 nm, then measured and irradiated the water/ethanol, water/TFE, and water/dioxane samples using the same procedure. The water/TFE and water/dioxane samples required longer total irradiation time than the water and water/ethanol samples. Due to time constraints, the maximum total irradiation time for any sample was 40 minutes, which was sufficient to decrease the absorbance of each sample by at least 30%.

3.3 CD correction for concentration differences

It was necessary to correct the CD spectra for concentration differences because we could not be sure about the precision of the sample size as given to us by Midland and because various factors during sample preparation prevented our precise knowledge of the concentration. We corrected the CD spectra for concentration differences according

to the equation

$$\Delta\epsilon_\lambda = \frac{\theta_\lambda}{32980\ b\ C} \tag{3.1}$$

where $\Delta\epsilon_\lambda$ is the circular dichroism at the wavelength λ, θ_λ is the experimental ellipticity, which is unitless, at λ, b is the pathlength through the sample in cm, and C is the concentration of the solute[67] in mol L^{-1}. We determined the concentration using the Beer-Lambert law, Equation (2.3), and the molar absorptivity used in the Beer-Lambert expression was determined to be 163.2 L $mmol^{-1}$ cm^{-1} at 260 nm by the nearest-neighbor method described by Cantor.[49]

3.4 Experimental precautions

We wanted to be sure that the results we obtained from my experiments were caused only by the variables we were interested in, so we spent some time thinking about experimental factors that had the potential to influence our data.

Certain solvents have a tendancy to dissolve rubbers and plastics, which leads to contamination of the sample. We had some concern that such a negative interaction between our solvents and the plastic of the vials provided by Midland might contaminate our samples, so we ran a number of tests using the aforementioned UV-Vis and CD spectrometers to ensure that this was not the case. Our procedure follows. We took normal absorption and CD measurements of each of the solvents we planned to use (water, ethanol, TFE, and dioxane), then we added 0.500 mL of the four solvents to each of four clean, plastic vials from Midland. After waiting 24 hours, we measured the steady-state absorbance and CD of the solvents from the vials and compared the spectra before and after interaction with the vials. Any possible interactions between the solvents and plastic were found to have negligible effects.

We were also concerned that ionic strength might affect our measurements. We

planned to use premade stock buffer solution which included 0.25 M Na^+ ions, but it has been shown by Boedtker[68] and McMullen *et al.*[69] that there is an increase in the helicity of certain types of RNA with an increase in ionic strength. We therefore prepared three solutions of $(dT)_{18}$ in buffered water with 0.0 M, 0.5 M, and 1.0 M NaCl, respectively. We took steady-state absorption and CD measurements of the solutions and found no dependence on either with ionic strength. In the end, this short experiment only fulfilled a curiosity; we ended up making our own buffer solution for our experiments.

A third concern of ours was the possibility that the UV light used in the absorption spectrometer might cause unwanted photodimerization in our samples. To ensure that this was not a problem, we made two samples using water as the solvent. We measured the steady-state absorbance of the first sample, thereby exposing it to brief UV irradiation. Next we measured the CD of both samples and found no difference in CD signal due to irradiation from the UV-Vis spectrometer. The reason this is not a concern is that the power of the UV light used in absorbance measurements is far too weak to cause significant photodimerization.

Chapter 4

Results and discussion

4.1 Solubility experiments

4.1.1 Results

The resulting absorbance spectra are shown in Figure 4.1. The graphs are plotted as source wavelenth in nm versus absorbance. Note that these raw data do not show a relationship between solvent and extent of base stacking; rather, they were used for the concentration corrections of the CD data. Although the same amount of solvent was added to each sample, the absorbance values vary widely and non-linearly with increasing co-solvent. This is probably because the vials from Midland did not contain equal amounts of $(dT)_{18}$. It is interesting to note that while $(dT)_{18}$ was insoluble in 100% ethanol and dioxane solutions, it was soluble in 100% TFE.

The CD spectra are shown in Figure 4.2. The data are plotted as $\Delta\epsilon$, change in circular dichroism, in mdeg M^{-1} cm^{-1}, versus excitation wavelength in nm. Again, it is apparent that as the percent of co-solvent increases, the circular dichroism signal decreases. We did not measure the CD of $(dT)_{18}$ in 100% dioxane due to its insolubility. Note that the CD signal of $(dT)_{18}$ in 75% TFE is very similar to the CD signal in 100%

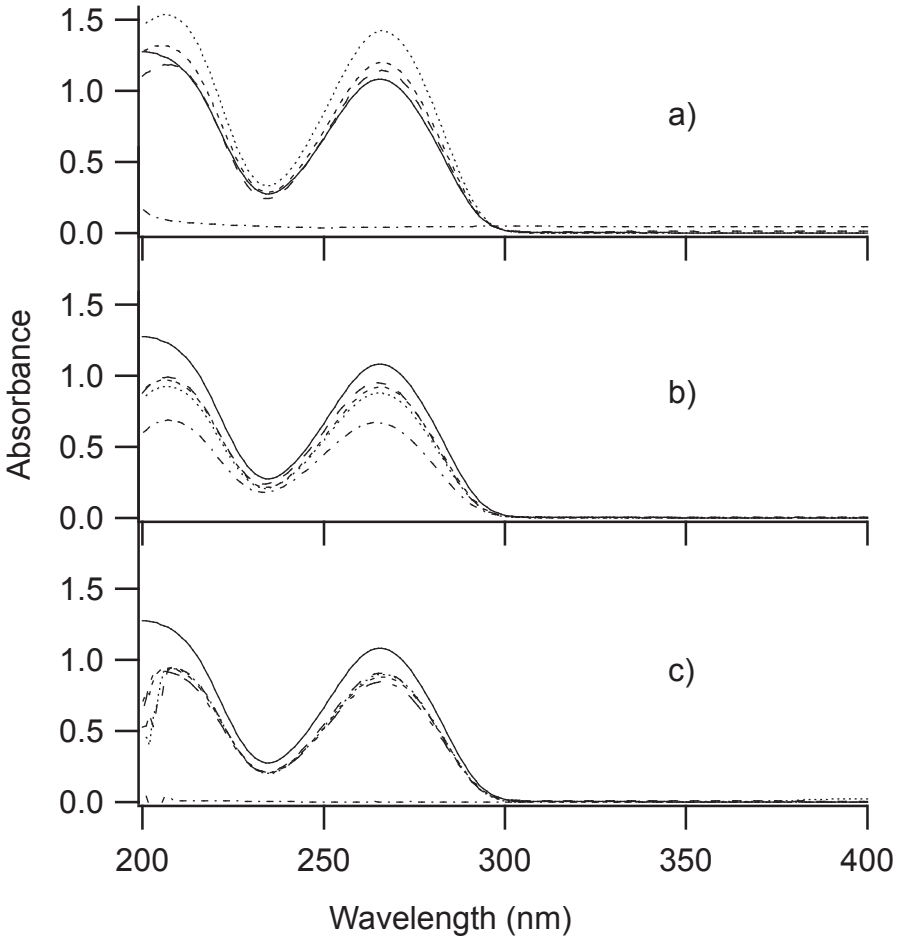

Figure 4.1: Absorption spectra of various percent mixtures of a) ethanol, b) TFE, and C) dioxane. Co-solvent concentrations are as follows: 0% (solid), 10% (dot, long dash), 25% (short dash), 50% (dots), 75% (long dash), 100% (dot, short dash); note that these raw data show no relationship between solvent and extent of base stacking.

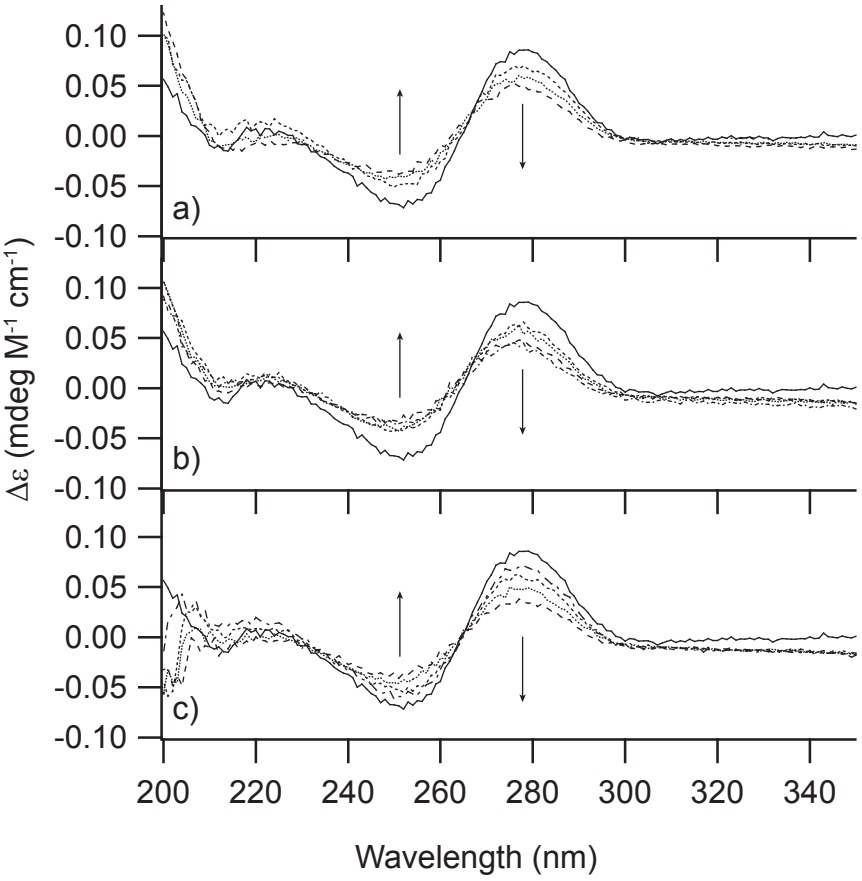

Figure 4.2: CD spectra of verious percent mixtures of a) ethanol, b) TFE, and c) dioxane. Co-solvent concentrations are as follows: 0% (solid), 10% (dot, long dash), 25% (short dash), 50% (dots), 75% (long dash), 100% (dot, short dash); the arrows show trends in CD changes with increasing % co-solvent.

TFE.

The maximum solvating concentrations of ethanol and dioxane were observed to be 75%. We expect that as the percent composition of ethanol and dioxane increase from 75%, the solubility of $(dT)_{18}$ falls off sharply at some maximum percent composition which is characteristic of each solvent. Unfortunately, due to a lack of sample material, it was not possible to take spectra of solutions with concentrations between 75% and 100%.

4.1.2 Discussion

There are two components of $(dT)_{18}$ that can give a CD signal. These are the ribose sugars and the chiral aggregations that result from base stacking interactions. The thymine bases themselves, which are symmetrical across the molecular plane, and the phosphate esters, which contain various symmetry elements, are achiral.

According to Johnson,[70] the different conformations of DNAs and RNAs (A, B, and Z) exhibit characteristic CD spectra for a given nucleotide sequence. Also, the conformation of the nucleotide depends on the conformation of the constituent ribose units. The CD spectra presented in Figure 4.2 show changes in the magnitudes of the bands but not in the positions of the band maxima and minima. Thus, there is not a change in the overall conformation of $(dT)_{18}$ depending on experimental conditions. Since the absorptive properties of the ribose sugars are not affected by solvent interactions, any differences seen in the CD spectra of $(dT)_{18}$ which depend on the solvent conditions are due to changes in the amount of base stacking in the molecule.

General conclusions

Again, look at Figure 4.2. Since only changes in the base stacking will lead to changes in the CD signal, the addition of each co-solvent to water must decrease base stacking

in the molecule.

Notice again that the CD signal for 75% TFE and the signal for 100% TFE are similar. Because the CD signal resulting from the ribose units is not dependent on the extent of base stacking and because the scans are identical to experimental precision, it could be surmised that the CD signals shown in these two scans are probably caused by the ribose sugars alone, with no contribution from stacked bases. However, we will show in the next section that upon irradiation, the CD signal for $(dT)_{18}$ in in 75% TFE decreases slightly further. This additional decrease may be evidence of the formation of the thymine (6-4) homoadduct or the thymine photohydrate, both of which are minor photoproducts.[71]

In this solubility study, we have determined that the maximum percents volume of ethanol, TFE, and dioxane in which $(dT)_{18}$ is soluble are 75%, 100%, and 75%, respectively. At the time of the radiation study, we were not able to explain the similarity between the CD signals of $(dT)_{18}$ in 75% and 100% TFE; we suspected at the time that the similarity was due to procedural error. Therefore, 75% TFE was used in the radiation studies for reasons of caution. More recently, we have surmised that this similarity in magnitude is due to complete unstacking of the oligomer in both the 75% and 100% TFE/water solutions. The solvent used for the radiation experiments of $(dT)_{18}$ in dioxane contained 75% co-solvent. Finally, because the 75% ethanol solvent was not visibly transparent, 50% ethanol solutions were used for the subsequent radiation study rather than 75% ethanol solutions.

Solvent effects on base stacking

By comparing the absorbance of $(dT)_{18}$ in various 50% co-solvent mixtures, it is possible to ascertain the relative denaturing effects of the co-solvents. Figure 4.3 shows the CD spectra of $(dT)_{18}$ dissolved in water and in the three co-solvent mixtures at 50% co-solvent. As you can see from Figure 4.3, the CD signals of $(dT)_{18}$ in the three 50%

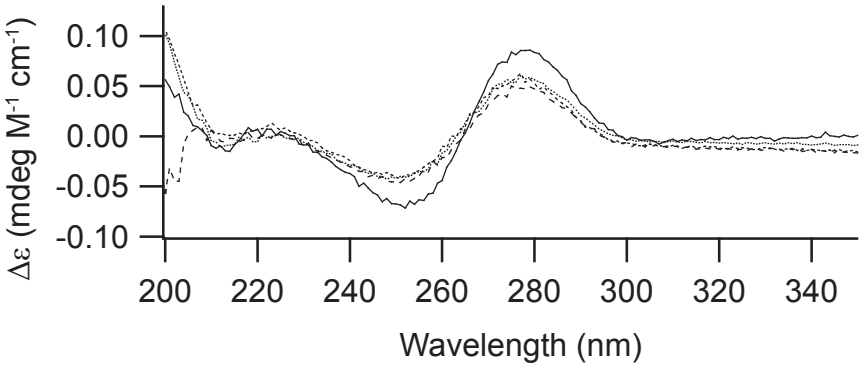

Figure 4.3: CD spectra of $(dT)_{18}$ in 50% mixtures of a) ethanol, b) TFE, and c) dioxane. Solvents are as follows: water (solid), ethanol (dots), TFE (short dash), dioxane (long dash).

Co-solvent	$\Delta\epsilon$ at 278 nm [mdeg M^{-1} cm^{-1}]	Denaturing efficiency (Relative to water solution)
Water	0.085713	1.000
50% Ethanol	0.057243	0.668
50% Trifluoroethanol	0.053961	0.630
50% Dioxane	0.047555	0.555

Table 4.1: Comparison of CD magnitude at 278 nm in 50% solutions of different co-solvents.

co-solvent mixtures are all very similar, and all less than the signal in water. However, there is some slight difference, and the $\Delta\epsilon$ value relative to water at 278 nm for each of these 50% solutions is shown in Table 4.1.2. Figure 4.4 shows the dependence of CD signal at the 278 nm maximum versus percent co-solvent. Exponential curves have been fit to the points, and the curve-fitting parameters are shown in Table 4.1.2, in which the fitting function is

$$\Delta\epsilon = K\ e^{-k\lambda} + \Delta\epsilon_0 \tag{4.1}$$

These data will be useful in the discussion of the radiation experiments, which are explained in the following section.

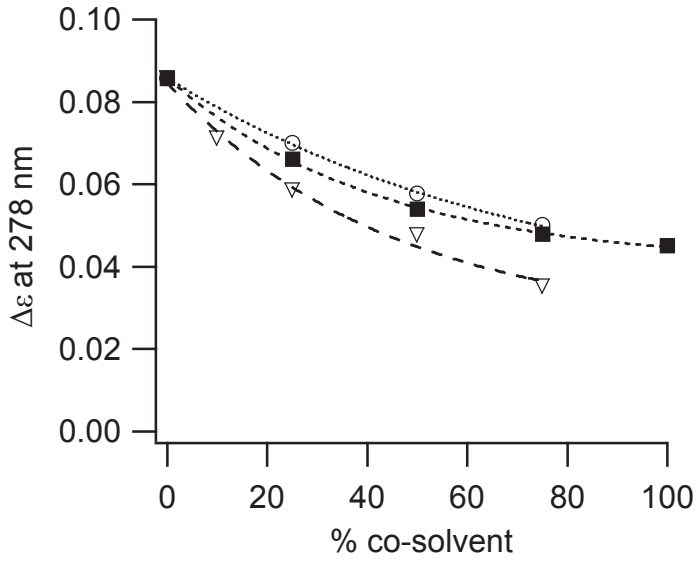

Figure 4.4: The CD at 278 nm vs. % co-solvent for ethanol (circles), TFE (squares), and dioxane (triangles) with exponential fits.

Co-solvent	K [M^{-1}]	k [nm^{-1}]	$\Delta\epsilon_0$ [M^{-1}]
Ethanol	0.056 ± 0.004	0.013 ± 0.001	0.029 ± 0.004
Trifluoroethanol	0.045 ± 0.001	0.023 ± 0.001	0.040 ± 0.001
Dioxane	0.059 ± 0.008	0.022 ± 0.007	0.025 ± 0.009

Table 4.2: Parameters for the exponential fit of CD signal at 278 nm versus percent co-solvent.

4.2 Radiation experiments

4.2.1 Results

Plots of the normal absorbance versus irradiation time for each solvent are shown in Figure 4.5. Of note are the decrease of absorbance at 266 nm and 210 nm with increasing

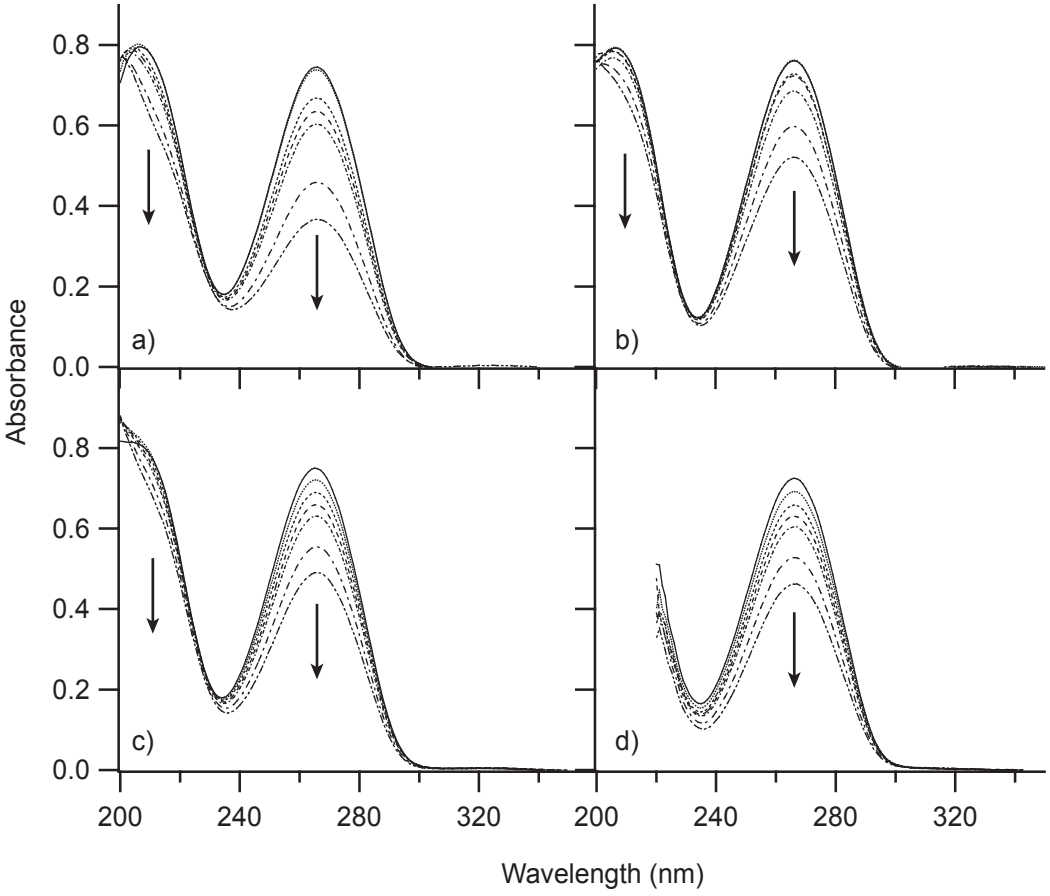

Figure 4.5: Absorbance vs. irradiation time for a) water, b) ethanol, c) TFE, and d) dioxane solutions. Irradiation times are as follows for a) and b): 0 min (solid), 0.5 min and 2 min (dots), 4 min (short dash), 6 min (long dash), 8 min (dot, short dash), 20 min (dot, long dash), 32 min (dot, dot, long dash). Irradiation times are as follows for c) and d): 0 min (solid), 4 min (dots), 8 min (short dash), 12 min (long dash), 16 min (dot, short dash), 28 min (dot, long dash), 40 min (dot, dot, long dash).

irradiation time for each solvent. The dioxane spectra were cut off at 220 nm due to

Co-solvent Co-solvent	k [min^{-1}]	A_0
Water	-0.01809 ± 0.00051	0.7445 ± 0.0025
50% Ethanol	-0.00853 ± 0.00066	0.7663 ± 0.0062
75% Trifluoroethanol	-0.00741 ± 0.00007	0.7487 ± 0.0007
75% Dioxane	-0.00756 ± 0.00024	0.7223 ± 0.0024

Table 4.3: Parameters for the linear fit of Absorbance at 266 nm versus time irradiated.

saturation of the detector (dioxane itself absorbs in this region).

Figure 4.6 shows the relationship between the absorbance at 260 nm and total time of irradiation. We have fit linear curves to the data, and the fit paramters are shown

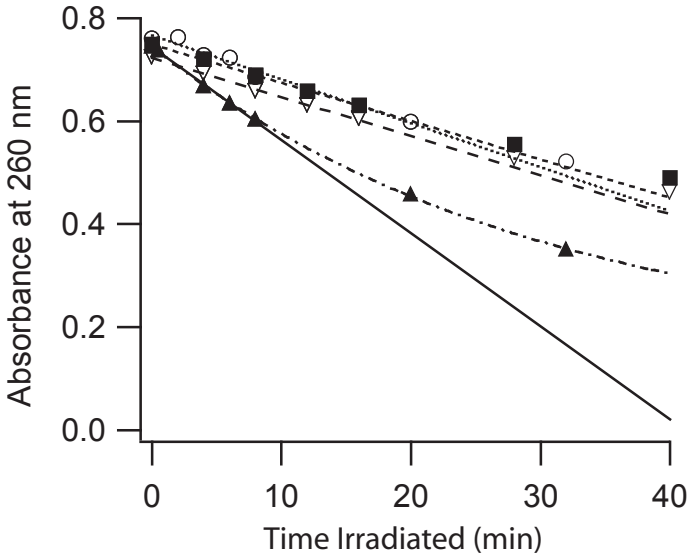

Figure 4.6: Absorbance at 260 nm in water (filled triangles; solid and dot, dash lines), ethanol (circles; dots), TFE (squares; short dash), and dioxane (empty triangles; long dash), with exponential fits.

in Table 4.2.1. The equation used for the fit was

$$A_{266} = kt_{irr} + A_0 \tag{4.2}$$

where only points with A values greater than 0.6 were included in the fit (in order to maintain consistency in comparing 25% degradation). As is shown by the graph,

the absorbance changes differently with radiation depending on which solvent is used. Although the decay of absorbance versus irradiation time can be expected to follow an exponential decay, linear fits were used. This is because with only a 25% decrease in absorbance, the data can be better fit to a line than to an exponential curve. However, as the exponential fit of the data for the water sample shows, with a greater decrease in absorbance the data exhibit an exponential decay.

Further informaion can be gained by examining the CD spectra. Figure 4.7 shows the CD spectra of each of the solvents at various irradiation times. All of the CD data were fit to five-term Gaussian functions of the form

$$y = \sum_{n=1}^{5} C_n \exp\left\{\frac{-(x - x_n)^2}{k_n}\right\}$$

strictly for fitting purposes (these are not theoretical calculations). The CD signal for dioxane has been cut off at wavelengths less than 240 nm because at this point, absorption of dioxane itself causes saturation of the detector and the signal to noise ratio becomes large.

4.2.2 Discussion

General Conclusions

As mentioned in the previous chapter, the only components of irradiated DNA that can give rise to CD effects are base stacks and ribose sugars. After irradiation, the photodimers created should also give rise to CD effects because an angle of 28.5° between the pyrimidine planes of the two thymine bases involved and a rotation of 28° between the two bases result in chirality of the photodimer.[72] Fortunately, Fenick *et al.* have shown that the thymine photodimer absorbs most strongly at wavelengths less than 200 nm.[73] Since CD is actually an absorption phenomenon and the photodimer absorbs

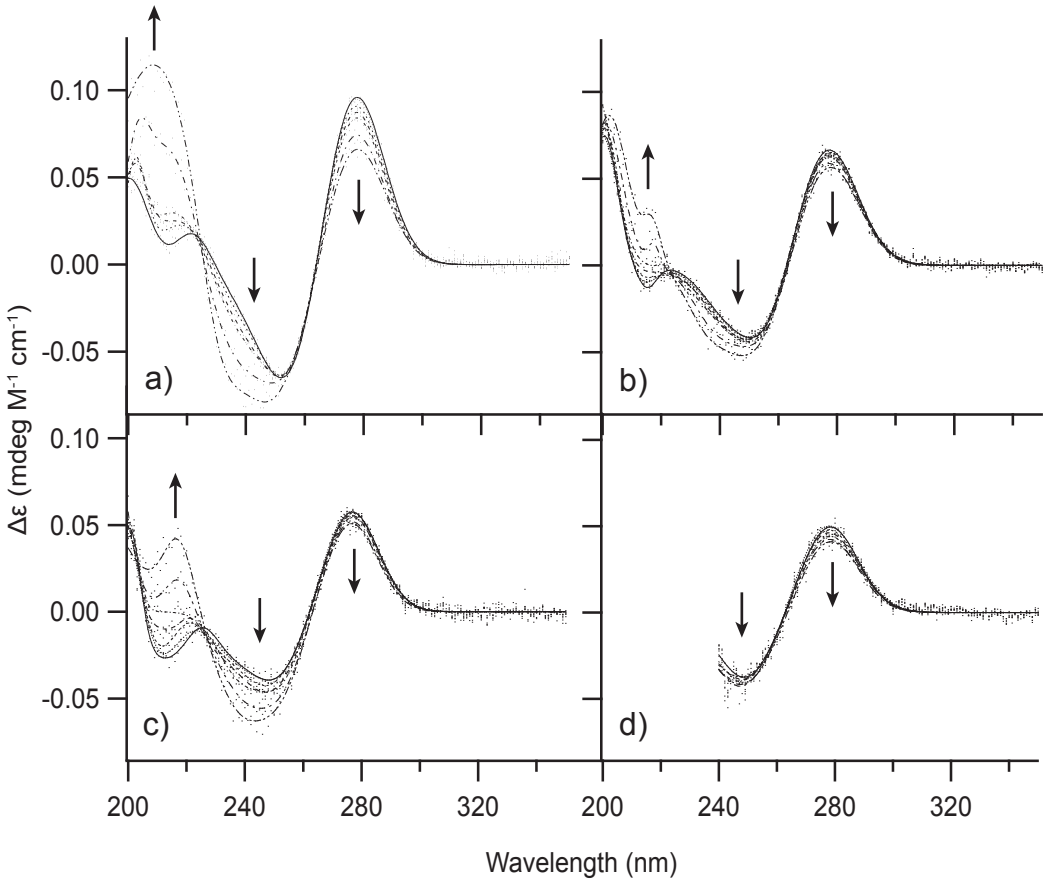

Figure 4.7: CD spectra at varying irradiation times for a) water, b) ethanol, c) TFE, and d) dioxane solutions. Irradiation times are as follows for a) and b): 0 min (solid), 0.5 min and 2 min (dots), 4 min (short dash), 6 min (long dash), 8 min (dot, short dash), 20 min (dot, long dash), 32 min (dot, dot, long dash). Irradiation times are as follows for c) and d): 0 min (solid), 4 min (dots), 8 min (short dash), 12 min (long dash), 16 min (dot, short dash), 28 min (dot, long dash), 40 min (dot, dot, long dash).

minimally at wavelengths greater than 250 nm, any change in intensity of the CD band at 277 nm is due only to photodegradation upon irradiation.

For a given percent of co-solvent, the decrease in intensity of the CD signal is due to the photodegradation of the sample. As is shown in Figure 4.7, the CD band at 277 nm decreases for every solvent as irradiation increases. We must keep in mind that while all of the solvents contribute to a decrease in CD signal as irradiation time increases, this decrease in CD signal occurs at different rates for each of the solvents. For example, in the water solution, an irradiation time of 10 minutes decreases the CD signal by 15%; in the ethanol solution, it takes 32 minutes to achive this percent decrease. Figure 4.8

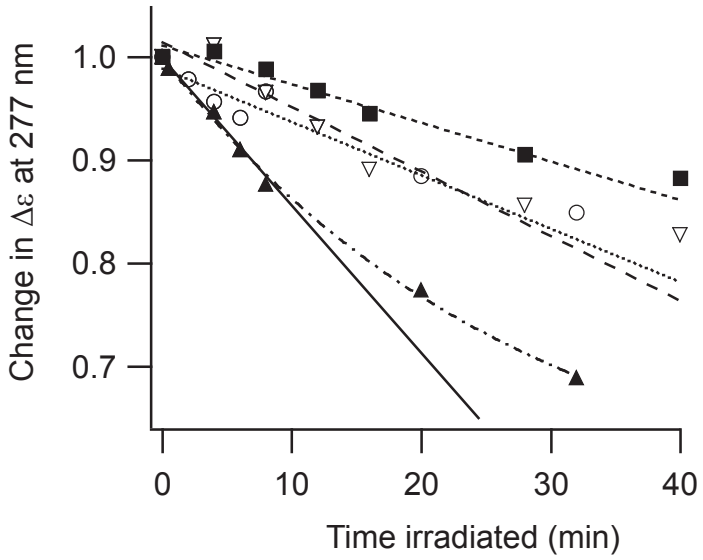

Figure 4.8: CD at 277 nm in water (filled triangles; solid and dot, dash lines), ethanol (circles; dots), TFE (squares; short dash), and dioxane (empty triangles; long dash).

shows this graphically, with linear fits based on the equation

$$\Delta\epsilon = kt_{irr} + \Delta\epsilon_0 \tag{4.3}$$

and the fit parameters shown in Table 4.2.2, where only points with $\Delta\epsilon$ values greater than 0.9 were included in the fit. Again, due to the small decrease in $\Delta\epsilon$, linear fits

Co-solvent	k [min^{-1}]	$\Delta\epsilon_0$ [M^{-1} cm^{-1}]
Water	-0.0143 ± 0.0009	0.999 ± 0.003
50% Ethanol	-0.0051 ± 0.0027	0.989 ± 0.013
75% TFE	-0.0037 ± 0.0039	1.011 ± 0.005
75% Dioxane	-0.0062 ± 0.0021	1.014 ± 0.016

Table 4.4: Parameters for the linear fit of CD at 277 nm versus time irradiated.

Co-solvent	$\Delta\epsilon$ at 278 nm [mdeg M^{-1} cm^{-1}]	Relative efficiency of Base Stacking*	k from linear fit	Relative Rate*
Water	0.085713	1.000	-0.0143	1.000
50% Ethanol	0.057243	0.668	-0.0051	0.356
75% TFE	0.047879	0.559	-0.0037	0.258
75% Dioxane	0.044291	0.517	-0.0062	0.433

Table 4.5: Relationship between denaturing efficiency of solvent and rate of photodegradation. *Relative to water solution.

were more appropriate than exponential fits. Although the errors for the parameters are large, the data suggest that the denaturing effects of the solvents play a significant part in the rate of formation of thymine photodimers.

Now we must relate the amount of base stacking as determined in the solubility experiments to the rate of decrease in CD signal at 277 nm with irradiation. For this, we must use efficiencies of base stacking similar to those shown in Table 4.1.2. The relationship between the denaturing power of a solvent and the rate of CD decrease is shown in Table 4.2.2. We expected the relationships between the rates of CD signal decrease to be similar to the relationship between the indeces of base stacking. While this general trend is followed, except in dioxane, the large errors associated with the linear fits makes any quantitative correlation difficult to justify.

Proof of photodimer formation

A simple subtraction process is all that is necessary to show that T<>T was formed during irradiation. Since the CD band around 280 nm is due only to base stacking and

the sugar residues, the absorption spectrum of T<>T can be estimated by normalizing the absorption spectra for each solvent before and after irradiation, then subtracting the two. Figure 4.9 shows the results for $(dT)_{18}$ in water. The main features of this plot

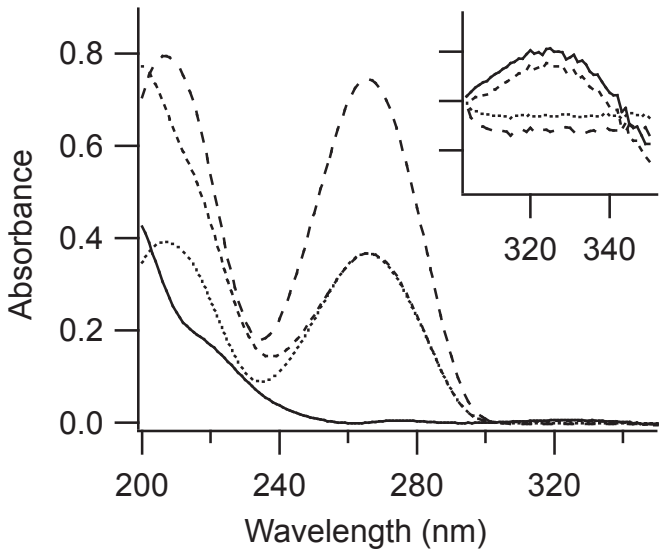

Figure 4.9: Absorption spectra for non-irradiated (long dash), scaled (dots), and irradiated (short dash) $(dT)_{18}$, and the photodimer spectrum (solid) resulting from subtraction). Inset: zoomed view of absorbance caused by thymine (6-4) homoadduct.

are the strong band at < 240 nm and the low-intensity band near 320 nm. The former is due to the actual photodimer and the latter is due to the thymine (6-4) homoadduct, a minor side-product of far-UV irradiation.[74] Figure 4.10 shows the T<>T spectra obtained by this method for $(dT)_{18}$ in all of the solvents except dioxane and includes the T<>T spectrum in water from Herbert, *et al.*,[73] which has been normalized to the water curve. All of the curves follow the same basic behavior, which shows that T<>T has been made. Unfortunately, the spectrum for dioxane was not included due to substantial noise at $\lambda < 220$ nm. Still, data show that the dioxane absorbance increases near 240 nm, matching the other spectra, and also exhibits a minor band at 320 nm, leading me to believe that the photochemistry in dioxane is similar to that in the other solvents. Also, we must keep in mind that this subtraction process only leads

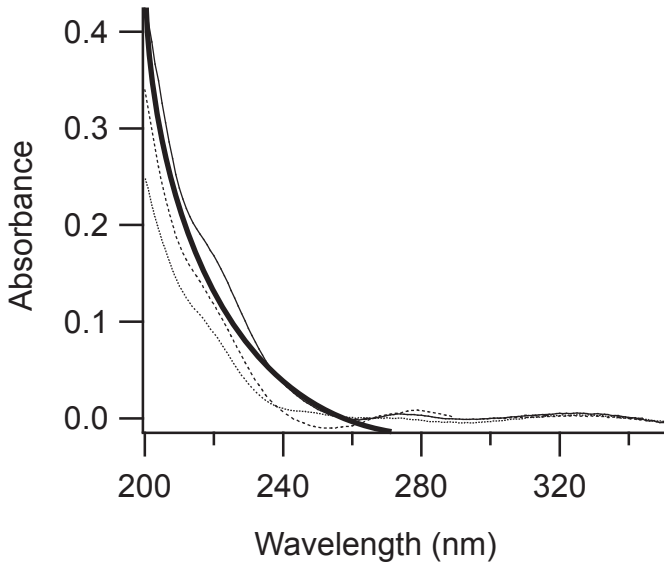

Figure 4.10: Absorption spectra photodimer spectrum resulting from subtraction in water (solid), ethanol (dots), and TFE (short dash). The thick line is from Herbert, 1969.

to an estimation of the photodimer absorption spectrum, which is why the experimental photodimer spectra do not exactly match the spectrum from Herbert.

4.3 Future Work

These few experiments are part of an ongoing project which should last through the summer and hopefully lead to a publication. With repeated runs of the experiments in the future, we will decrease the noise associated with the CD spectra, strengthen our results by showing repeatability, and decrease the large errors associated with the exponential fit listed in Table 4.2.2. As the experiment stands, much evidence suggests that our hypothesis is correct, but the results are inconclusive. Repeated trials should increase the precision of our measurements and improve confidence in our results.

Any conclusions drawn from this data are dependent upon the truth of a fairly large assumption that we had to make at this point in my work, namely, that the photodynamics of the excited thymine residues is the same in the various solvents.

This is not an unreasonable assumption; as stated by Hare,[75] the singlet (S_1) lifetime for 1-cyclohexyluracil, a derivative of uracil, was found to be equal in different solvents within experimental uncertainty. In order to prove that this is the case for $(dT)_{18}$, time-resolved transient absorption spectroscopy experiments must be carried out. Work in that direction is in progress.

Chapter 5

Conclusions

The rate of photodimerization in $(dT)_{18}$ was studied as a function of the relative denaturing efficiency of various solvents. The trends shown in this study are very encouraging. The solubility experiments have shown that the maximum percents volume of co-solvent in which $(dT)_{18}$ is soluble are 75%, 100%, and 75% for ethanol, TFE, and dioxane, respectively. Also, the denaturing efficiencies of these solvents relative to water are 0.668, 0.559, and 0.517, respectively. The irradiation experiments have shown that the rates of photodegradation for these solvents relative to water are 0.356, 0.258, and 0.433, respectively. A correllation between the denaturing efficiency of the solvents and the rate of photodimerization of $(dT)_{18}$ in solutions of these solvents (except dioxane) provide qualitative proof that base stacking can have a dramatic effect on photodimerization. These conclusions make sense considering the ultrafast fluorescence decay exhibited by excited thymine residues. With additional experiments, errors will be reduced and these results will be made quantitative.

The deleterious effects of thymine photodimerization were discovered nearly fifty years ago, and work is still being done to understand the mechanistic process behind the photoreaction. With our present work, we add to the knowledge of the scientists who came before us.

Bibliography

[1] Blackburn, G. M.; Davies, R. J. H. *Biochem. Biophys. Res. Commun.* **1966,** *22,* 704–706.

[2] Sancar, A.; Sancar, G. B. *Ann. Rev. Biochem.* **1988,** *57,* 29-67.

[3] Avery, O.; MacLeod, C.; McCarty, M. *J. Expt. Med.* **1944,** *79,* 137-157.

[4] Miescher, J. F. *Hoppe-Seylers medicinisch-chemische Untersuchungen* **1871,** *4,*.

[5] Freifelder, D., Ed.; *The DNA Molecule: Structure and Properties: Original Papers, Analyses, and Problems;* W. H. Freeman and Company: San Francisco, 1978.

[6] Altman, R. *Arch. Anat. Physiol., Physiol. Abt.* **1889,** 524.

[7] Kossel, A. *Arch. Anat. Physiol., Physiol. Abt.* **1891,** 181.

[8] Levene, P. A.; Jacobs, W. A. *Ber. Deut. Chem. Ges.* **1908,** *41,* 2703.

[9] Levene, P. A.; Mori, T. *J. Biological Chem.* **1929,** *83,* 793.

[10] Carey, F. A. *Organic Chemistry;* McGraw Hill: Boston, Fifth ed.; 2003.

[11] Olby, R. *The Path to the Double Helix;* University of Washington Press: Seattle, 1974.

[12] Vischer, E.; Zamenhof, S.; Chargaff, E. *J. Biological Chem.* **1949,** *177,* 429-438.

[13] Chargaff, E. *Experientia* **1950,** *6,* 201–209.

[14] Campbell, N. A.; Reece, J. B. *Biology;* Benjamin Cummings: San Francisco, Sixth ed.; 2002.

[15] Bloomfield, V. A.; Crothers, D. M.; Tinoco Jr., I. *Nucleic Acids: Structures, Properties, and Functions;* University Science Books: Sausalito, California, 2000.

[16] Saenger, W. *Principles of Nucleic Acid Structure;* Springer-Verlag New York Inc.: New York, 1984.

[17] Pauling, L.; Corey, R. B. *Proc. U.S. Nat. Acad. Sci.* **1953,** *39,* 84.

[18] Watson, J. D.; Crick, F. H. C. *Nature* **1953,** *171,* 737-738.

[19] Furberg, S. *Acta Chem. Scand.* **1952,** *6,* 634.

[20] Wyatt, G. R. *J. Gen. Physio.* **1952,** *36,* 201–205.

[21] Ts'o, P. O. P. Bases, Nucleosides, and Nucleotides. In *Basic Principles in Nucleic Acid Chemistry*, Vol. I; Ts'o, P. O. P., Ed.; Academic Press, Inc.: New York, 1974.

[22] Franks, F. The hydrophobic interaction. In *Water, a Comprehensive Treatise*; Franks, F., Ed.; Plenum Press: New York, 1975.

[23] Crothers, D. M.; Ratner, D. I. *Biochemistry* **1968,** *7,* 1823-1827.

[24] Tazawa, I.; Koike, T.; Inoue, Y. *Eur. J. of Biochem.* **1980,** *109,* 33–38.

[25] London, F. *Z. Phys. Chem. Abt. B* **1930,** *11,* 222-251.

[26] Haasnoot, C. A. G.; Altona, C. *Nuc. Acids Res.* **1979,** *6,* 1135–1149.

[27] Pörschke, D. *Eur. J. of Biochem.* **1973,** *39,* 117-126.

[28] Reich, C.; Tinoco Jr., I. *Biopolymers* **1980,** *19,* 833–848.

[29] McQuarrie, D. A.; Simon, J. D. *Physical Chemistry: A Molecular Approach;* University Science Books: Sausalito, CA, 1997.

[30] Marguet, S.; Markovitsi, D. *J. Am. Chem. Soc. Commun.* **2005,** *127,* 5780–5781.

[31] Crespo-Hernández, C.; Cohen, B.; Kohler, B. In press, 2005.

[32] Gueron, M.; Eisinger, J.; Lamola, A. A. Excited States of Nucleic Acids. In *Basic Principles in Nucleic Acid Chemistry*, Vol. I; Ts'o, P. O. P., Ed.; Academic: New York, 1974.

[33] Beukers, R.; Ijlstra, J.; Berends, W. *Rec. Trav. Chim.* **1960,** *79,* 101.

[34] Rörsch, A.; Barkes, R.; Ijlstra, J.; Berends, W. *Rec. Trav. Chim. Pays Bas.* **1958,** *77,* 423–429.

[35] Beukers, R.; Berends, W. *Biochim. Biophys. Acta* **1960,** *41,* 550–557.

[36] Wang, S. Y. *Nature (London)* **1960,** *188,* 844–846.

[37] Wacker, A.; Dellweg, H.; Weinblum, D. *Naturwissenschaften* **1960,** *47,* 477.

[38] Fahr, E. *Angew. Chem. Int. Ed. Engl.* **1969,** *8,* 578–594.

[39] Fisher, G. J.; Johns, H. E. Pyrimidine Photodimers. In *Photochemistry and Photobiology of Nucleic Acids*, Vol. 1; Wang, S. Y., Ed.; Academic Press: New York, 1976.

[40] Johns, H. E.; Rappaport, S. A.; Delbrück, M. *J. Mol. Biol.* **1962,** *4,* 104.

[41] Johns, H. E. *et al. J. Mol. Biol.* **1962,** *9,* 104.

[42] Freeman, K. B.; Hariharan, P. V.; Johns, H. E. *J. Mol. Biol.* **1965,** *13,* 833–848.

[43] Pearson, M. L.; Ottensmeyer, F. P.; Johns, H. E. *Photochem. Photobiol.* **1965,** *4,* 731–747.

[44] Brown, I. H.; Johns, H. E. *Photochem. Photobiol.* **1968,** *8,* 273–286.

[45] Hariharan, P. V.; Johns, H. E. *Can J. Biochem.* **1968,** *46,* 911–918.

[46] Cadet, J. *et al. Can J. Chem.* **1985,** *63,* 2861–2868.

[47] Kemmink, J. *et al. Eur. J. Biochem.* **1987,** *162,* 37–43.

[48] Taylor, J.-S.; Brochie, I. R.; O'Day, C. L. *J. Am. Chem. Soc.* **1987,** *109,* 6735–6742.

[49] Cantor, C. R. *et al. Biopolymers* **1970,** *9,* 1059–1077.

[50] Girod, J. C. *et al. Biochemistry* **1973,** *12,* 5092–5096.

[51] Pettegrew, J. W.; Miles, D. W.; Eyring, H. *Proc. Natl. Acad. Sci. USA* **1977,** *74,* 1785–1788.

[52] Steely Jr., H. T.; Gray, D. M.; Ratliff, R. L. *Nuc. Acids Res.* **1986,** *14,* 10071–10090.

[53] Lamola, A. A.; Mittal, J. P. *Science* **1966,** *154,* 1560.

[54] Greenstock, C. L. *et al. Biochem. Biophys. Res. Commun.* **1967,** *27,* 431.

[55] Lisewski, R.; Wierzchowski, K. L. *Chem. Commun.* **1969,** 348.

[56] Morrison, H.; Feely, A.; Kloepfer, R. *Chem. Commun.* **1964,** 358.

[57] Steele, R. H.; Szent-Györgyi, A. *Proc. Nat. Acad. Sci. U.S.* **1957,** *43,* 477.

[58] Sutherland, B. M.; Sutherland, J. C. *Biopolymers* **1970,** *9,* 639.

[59] Whillans, D. W. *et al. Biochem. Biophys. Res. Commun.* **1969,** *36,* 912.

[60] Eisinger, J.; Lamola, A. A. *Biochem. Biophys. Res. Commun.* **1967,** *28,* 558.

[61] Markovitsi, D.; Sharonov, A.; Onidas, D.; Gustavsson, T. *ChemPhysChem* **2003,** *4,* 303.

[62] Durbeej, B.; Eriksson, L. A. *J. Photochem. and Photobiol. A* **2002,** *152,* 95–101.

[63] Durbeej, B.; Eriksson, L. A. *Photochem. and Photobiol.* **2003,** *78(2),* 159–167.

[64] Johnson Jr., C. W. Circular Dichroism Instrumentation. In *Circular Dichroism and the Conformational Analysis of Biomolecules*; Fasman, G. D., Ed.; Plenum Press: New York, 1996.

[65] Skoog, D. A.; Holler, F. J.; Nieman, T. A. *Principles of Instrumental Analysis;* Thomson Learning, Inc.: United States, Fifth ed.; 1998.

[66] Levine, L.; Gordon, J. A.; Jences, W. P. *Biochemistry* **1963,** *2,* 168–175.

[67] Crespo-Hernández, C. E.; Kohler, B. *J. Phys. Chem. B* **2004,** *108,* 11182.

[68] Boedtker, H. *J. Mol. Biol.* **1960,** *2,* 171.

[69] McMullen, D. W.; Jaskunas, S. R.; Tinoco Jr., I. *Biopolymers* **1967,** *5,* 589.

[70] Johnson Jr., C. W. Determination of the conformation of nucleic acids by electronic CD. In *Circular Dichroism and the Conformational Analysis of Biomolecules*; Fasman, G. D., Ed.; Plenum Press: New York, 1996.

[71] Fisher, G. J.; Johns, H. E. Pyrimidine Photohydrates. In *Photochemistry and Photobiology of Nucleic Acids*, Vol. 1; Wang, S. Y., Ed.; Academic Press: New York, 1976.

[72] Camerman, N. *Science* **1968,** *160,* 1451–1452.

[73] Herbert, M. A. *et al. Photochem. and Photobiol.* **1969,** *9,* 33.

[74] Wang, S. Y. Pyrimidine bimolecular photoproducts. In *Photochemistry and Photobiology of Nucleic Acids*, Vol. 1; Wang, S. Y., Ed.; Academic Press: New York, 1976.

[75] Hare, P.; Kohler, B. Private correspondence dated 5/20/2005.